

Electronic Supplementary Information for

Unraveling the peculiar *modus operandi* of a new class of solvatochromic fluorescent molecular rotors by spectroscopic and quantum mechanical methods

Matthias Koenig,^a Giovanni Bottari,^{*b} Giuseppe Brancato,^{*c} Vincenzo Barone,^c Dirk M. Guldi,^{*a} and Tomás Torres^b

^a Department of Chemistry and Pharmacy and Interdisciplinary Center for Molecular Materials (ICMM), Friedrich-Alexander-Universität Erlangen-Nürnberg, 91058 Erlangen, Germany. Fax: +49.9131.85-28307; Tel: +49.9131.85-27341; E-mail: dirk.guldi@uni-erlangen.de

^b Organic Chemistry Department, Universidad Autónoma de Madrid, 28049 Cantoblanco, Spain and IMDEA-Nanociencia, c/Faraday 9, Campus de Cantoblanco, 28049 Madrid, Spain. Fax: +34 914 973 966; Tel: +34 914 972 777; E-mail: giovanni.bottari@uam.es

^c Scuola Normale Superiore, Piazza dei Cavalieri 7, I-56126 Pisa, Italy and Istituto Nazionale di Fisica Nucleare, Largo Pontecorvo 3, I-56100 Pisa, Italy. Fax: +39 050 563513; Tel: +34 050 509071; E-mail: giuseppe.brancato@sns.it

Abbreviations

m.p. = melting point, NMR = nuclear magnetic resonance, ppm = parts per million, TLC = thin layer chromatography, BNAP = 2,2'-bis(diphenylphosphino)-1,1'-binaphthyl, dba = dibenzylideneacetone, DPAP = 4-(diphenylamino)-phthalonitrile

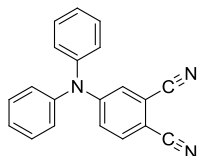
Materials and Methods

Chemicals and solvents were purchased from Aldrich and used without further purification. Dry toluene was freshly distilled under argon over an appropriate drying agent before use. M.p. were determined in a Büchi 504392-S equipment and are uncorrected. NMR spectra (¹H and ¹³C) were recorded with a Bruker Advance 300 MHz instrument. Chemical shifts values (δ) are referred to TMS, utilized as internal reference, t = triplet, d = doublets, dd = doublets of doublets, m = multiplet. IR spectra were recorded on a Bruker Vector 22 spectrophotometer employing in all cases solid samples (KBr pressed disks). EI-MS spectra were obtained from a VG AutoSpec spectrometer. Column chromatography was carried out on silica gel Merck-60 (230-400

mesh, 60Å). Analytical TLC was performed on aluminium sheets precoated with silica gel 60 F-254 from Merck.

Synthesis of 4-(diphenylamino)-phthalonitrile (DPAP)

Chemicals and solvents used for the preparation of **DPAP** were purchased from Aldrich and used without further purification. Dry toluene was freshly distilled under argon over an appropriate drying agent before use. 4-iodophthalonitrile (0.393 mM), diphenylamine (0.590 mM), Pd₂(dba)₃ (0.010 mM), Cs₂CO₃ (0.590 mM), and BINAP (0.010 mM) were put in a round-bottom flask and dry toluene (10 mL) was added. The solution was then stirred for 18 hrs under reflux. The reaction mixture was then cooled down to RT, the solvent removed, and the crude subjected to column chromatography on silica gel (CH₂Cl₂) obtaining **DPAP** as a yellow solid. Yield: 80%.



m.p.: 136-138 °C; ¹H NMR (300 MHz, CDCl₃, 25 °C) δ (ppm): 7.47 (d, J_{H-H} = 8.2 Hz, 1H), 7.45-7.35 (m, 4H), 7.26 (t, J_{H-H} = 8.0 Hz, 2H), 7.17 (d, J_{H-H} = 8.1 Hz, 4H), 7.15 (m, 1H), 7.09 (dd, J_{H-H} = 8.2 Hz, J_{H-H} = 1.8 Hz, 1H); ¹³C NMR (75.5 MHz, CDCl₃, 25 °C) δ (ppm): 151.6, 144.4, 134.3, 130.3, 126.6, 126.5, 121.9, 121.1, 116.7, 116.3, 115.6, 104.1; FT-IR (KBr) ν (cm⁻¹) 3077, 2221 (-CN), 1595, 1498 (C=C), 1326 (C-N), 1197, 1132, 817, 751, 716; EI (m/z): 295.3 [M]⁺ (100%).

Preparation of DPAP embedded in a poly(methyl methacrylate) (PMMA) matrix

A PMMA matrix containing DPAP was prepared by dissolving 0.3 g of PMMA and 0.016 g of **DPAP** in 3.2 ml of methyl methacrylate. This solution was then dripped onto a glass slide to obtain layers of different thicknesses and dried for several hours to vaporize the methyl methacrylate. Before used, all glass slides were rinsed several times with diluted sulfuric acid, distilled water, acetone, and again distilled water before they were finally dried at high temperatures (80–100 °C).

Growth of single crystals of DPAP for X-ray determination

Single crystals of **DPAP** suitable for X-ray diffraction studies were obtained by slow evaporation of a solution of **DPAP** in dichloromethane.

X-ray diffraction studies

The data were collected on a Bruker Smart 6000 diffractometer with a CCD area detector using a graphite monochromator with CuK α radiation ($\lambda = 1.54178 \text{ \AA}$). The data were collected at 100 K using an Oxford Cryosystem low temperature device. Data reduction was performed using the Bruker Smart. The structure was solved by direct methods using SHELXTL-97 and refined by full-matrix least-squares on F^2 with anisotropic displacement parameters for the non-H atoms using SHELXL-97.¹ The function, $\sum w(|F_o|^2 - |F_c|^2)^2$, was minimized, where $w = 1/[(\sigma(F_o))^2 + (0.0459*P)^2 + (11.7963*P)]$ and $P = (|F_o|^2 + 2|F_c|^2)/3$. Definitions used for calculating $R(F)$, $R_w(F^2)$ and the goodness of fit, S , are given below.² Neutral atom scattering factors and values used to calculate the linear absorption coefficient are from the International Tables for X-ray Crystallography (1992).³ The figure was generated using the ORPEP program.

Photophysical and electrochemical studies

All solvents were spectroscopic grade and were purchased from various commercial suppliers (Sigma-Aldrich, Merck and Roth). Dielectric constants, refractive indices, and viscosities of the pure solvents were obtained from the literature.⁴ UV/vis spectra were recorded with a Perkin Elmer Lambda 2 instrument and steady-state emission with a FluoroMax 3 fluorometer by HORIBA JobinYvon using a quartz cell with 10 mm optical path length. For emission below room temperature, a Haake KT40 thermostat/cryostat was installed, while for emission above room temperature samples were heated using a Haake NB22 thermostat. Fluorescence lifetimes were determined by using time-correlated single-photon counting (TCSPC) on a FluoroLog 3 emission spectrometer (Horiba JobinYvon). For excitation, a NanoLED 295 nm light source was used. The FluoroLog 3 instrument was also used to detect emission in the NIR-region. Femtosecond transient absorption studies were performed in argon-saturated solutions with 387 nm excitation laser pulses (1 kHz, 150 fs pulse width) from an amplified Ti:Sapphire laser system (Clark-MXR Inc.) with a laser energy of 200 nJ. Nanosecond laser flash photolysis experiments were carried out with argon or oxygen purged samples using a 355 nm laser pulse from a Quanta-Ray CDR Nd:Yag system (6 ns pulse width) in a front face excitation geometry. The electrochemical studies (cyclovoltammetry and square wave voltammetry) were performed in argon-saturated acetonitrile solutions with a EG&G Princeton Applied Research Model 263A

potentiostat/galvanostat using a one-compartment cell with a three electrode configuration. A glassy carbon electrode was used as the working electrode, a platinum wire as the counter electrode, and an Ag wire as the reference electrode. All solutions contained 0.1 M tetrabutylammonium hexafluorophosphate (TBAPF6) as supporting electrolyte. Spectroelectrochemical experiments were carried out with a setup containing an Analytik Jena Specord S 600 UV/vis spectrometer, a HEKA elektroniks PG 284 potentiostat, and a home-made cell with a three-electrode configuration. As working electrode a light-transparent platinum gauze was used, whereas a platinum plate and a Ag wire served as counter electrode and reference electrode, respectively. All spectroelectrochemical measurements were done in argon-saturated acetonitrile containing 0.2 M TBAPF6 as supporting electrolyte.

Computational details

Quantum mechanical (QM) calculations of the structural and optical properties of DPAP have been carried out by methods rooted into density functional theory (DFT) and its time-dependent extension (TD-DFT).⁵ As shown in previous studies, hybrid functionals (here B3LYP)⁶ and their long-range corrected extensions (here CAM-B3LYP)⁷ are especially appropriate for describing molecular systems with an extended electronic delocalization and their electronic excitations, at least when transitions with a long-range and non-overlapping charge transfer character are not involved. The modified triple-zeta SNST basis set⁸ has been used in all calculations. Solvent effects have been included by means of the conductor-like version of the Polarizable Continuum Model (C-PCM).⁹ Vertical transition energies have been computed within the usual linear response approximation in case of optical absorption, whereas a state-specific PCM calculation has been carried out for optical emission calculations.¹⁰ In the latter case, molecular structures corresponding to the first singlet excited state have been relaxed before emission calculations using analytical gradients.¹¹ Triplet state energies and geometries have been also computed to better interpret experiments. All quantum mechanical calculations have been carried out with the Gaussian09 software package.¹²

Table S1 This table resumes some physical properties of the solvents and PMMA matrix used in this study such as the dielectric constant (ϵ), the refractive index of the solvent (n) and the Lippert-Mataga solvent parameter (Δf)¹³ as well as the fluorescent quantum yield (Φ_f), emission lifetime (τ_f), radiative (k_R) and non-radiative (k_{NR}) decay constant for **DPAP** in the listed solvents. The solvents in the table are organized from the lower (top) to the higher (bottom) Δf values.

Solvent	n	ϵ	Δf	Φ_f	τ_f (ns)	k_R (ns ⁻¹)	k_{NR} (ns ⁻¹)
cyclohexane	1.426	2.023	0	0.42	9.16	0.0459	0.0633
<i>o</i> -xylene	1.496	2.568	0.0295	0.38	12.5	0.0304	0.0496
anisole	1.518	4.33	0.1122	0.24	14.45	0.0166	0.0526
tetrahydrofuran	1.407	7.52	0.2089	0.18	12.9	0.0140	0.0636
dichloromethane	1.424	8.93	0.2172	0.165	13.8	0.0120	0.0605
benzonitrile	1.53	25.2	0.2348	0.098	8.93	0.0110	0.1010
<i>n</i> -hexanol	1.418	13.3	0.2430	0.045	4.69	0.0096	0.2036
methyl isopropyl ketone	1.39	12.4	0.2502	0.068	8	0.0085	0.1165
dimethylsulfoxide	1.477	48	0.2642	0.012	1.61	0.0075	0.6137
dimethylformamide	1.43	37	0.2754	0.021	2.87	0.0073	0.3411
ethylene glycol	1.432	41.4	0.2761	0.0025	0.35	0.0071	2.8500
acetonitrile	1.344	37.5	0.3055	0.0155	2.61	0.0059	0.3772
methanol	1.326	33.8	0.3102	0.0021	0.58	0.0036	1.7205
PMMA matrix*	1.491	3.1	0.0671	0.23	12.3	0.019	0.063

* PMMA matrix has not been included in the Δf plots

$$\Delta f = \frac{\epsilon - 1}{2\epsilon + 1} - \frac{n^2 - 1}{2n^2 + 1} \quad (\text{eq. S1})$$

In eq. S1, which allows to calculate the Lippert-Mataga solvent parameter Δf , ϵ is the dielectric constant and n is the refractive index of the solvent.

Table S2 Lippert-Mataga polarity parameter (Δf) and non-radiative decay constants k_1 and k_2 as determined from transient absorption spectroscopy for **DPAP** in various solvents.

Solvent	Δf	k_1 (ns ⁻¹)	k_2 (ns ⁻¹)
<i>o</i> -xylene	0.0295	7.9	0.12
tetrahydrofurane	0.2089	7.2	0.15
acetonitrile	0.3055	12.4	0.31
methanol	0.3102	21.7	1.95

Table S3 Non-radiative decay constants k_1 and k_2 as determined from transient absorption spectroscopy for **DPAP** in solvents and solvents mixtures presenting different viscosity η .

Solvent	η (cP)	k_1 (ns ⁻¹)	k_2 (ns ⁻¹)
methanol	1.33	21.7	1.95
ethylene glycol	16.9	24	1.8
ethylene glycol/glycerine (1:1)	115	11.5	1.5
glycerine	1179	6.7	0.6

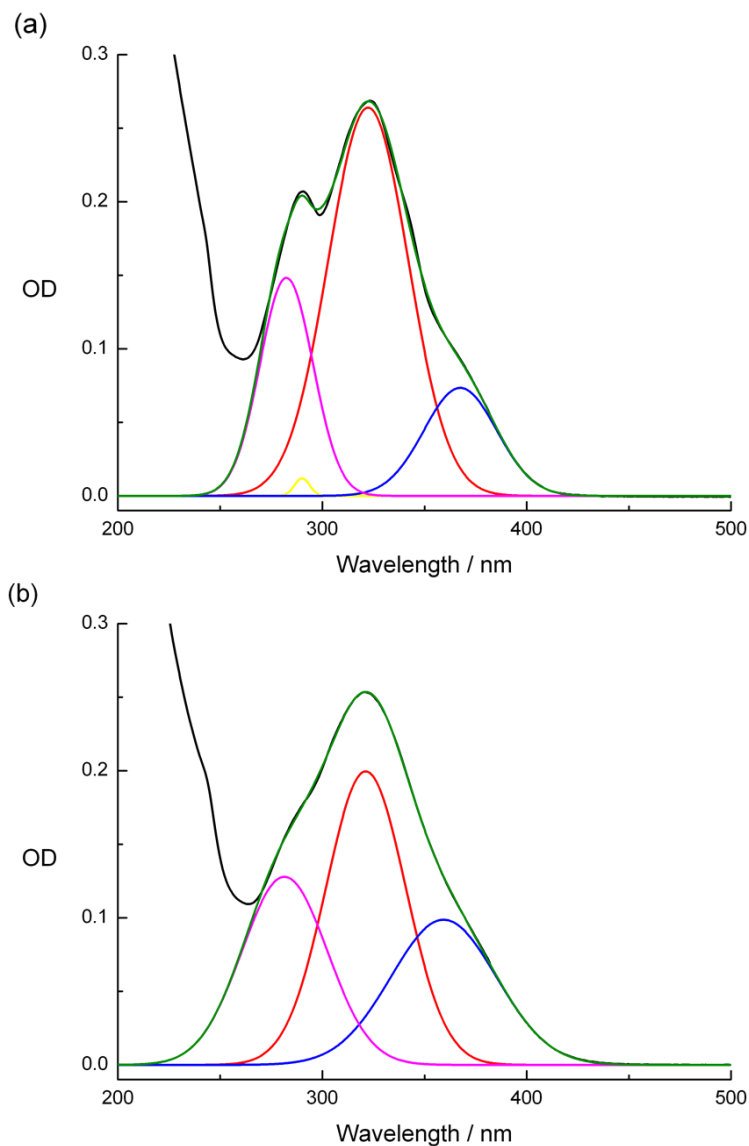


Fig. S1 Deconvolution of the absorption spectra (black) of **DPAP** in (a) cyclohexane and (b) acetonitrile. Shown are the three lowest-lying optical transitions (blue, red and magenta) and their sum fit (green). (Note that an additional Gauss-component (yellow) was needed in (a) to obtain a suitable sum fit)

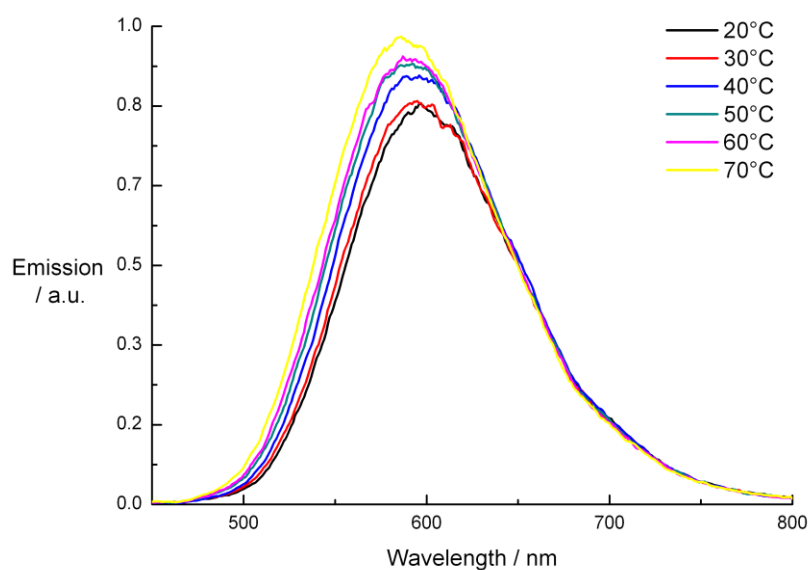


Fig. S2 Emission of **DPAP** (1×10^{-5} M) in DMF while increasing the temperature from 293 K (black) to 343 K (yellow) in 10 K steps. Excitation was at 328 nm.

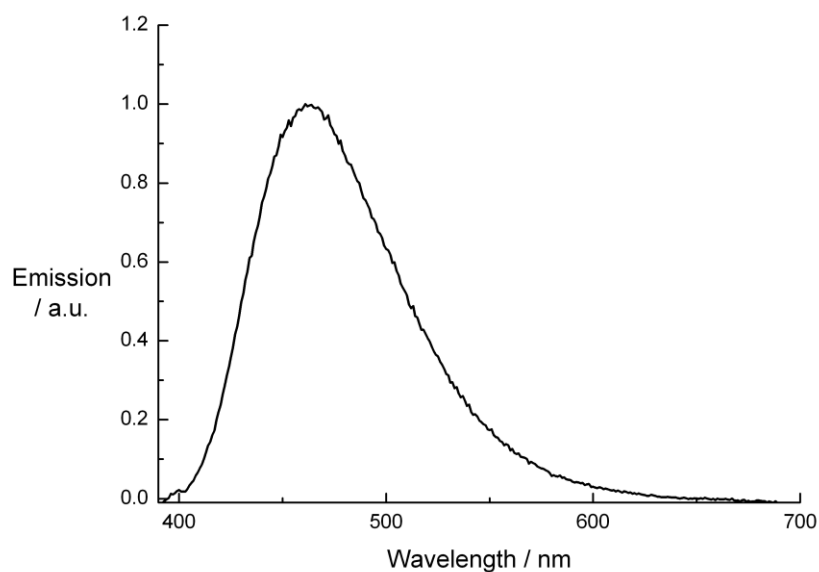


Fig. S3 Emission spectrum ($\lambda_{\text{exc}} = 354$ nm) of **DPAP** in a PMMA matrix on a glass slide.

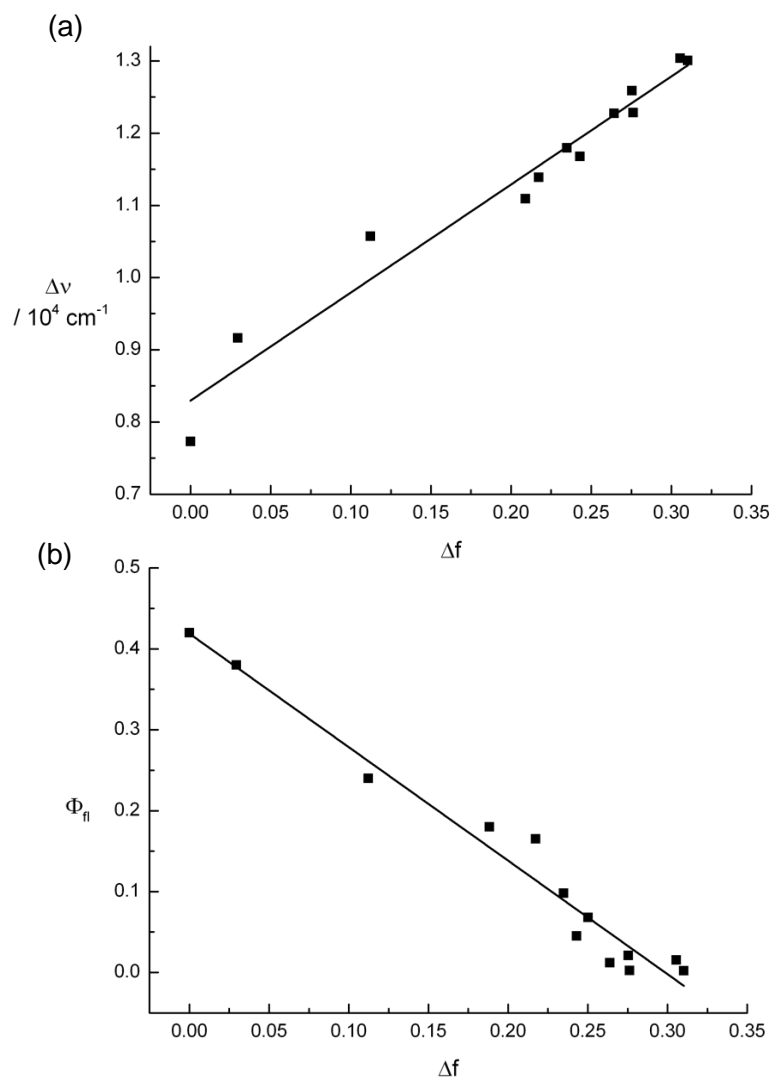


Fig. S4 (a) Lippert plot of **DPAP** as a function of the solvent parameter Δf and (b) plot of the Lippert-Mataga solvent parameter Δf versus the fluorescence quantum yield Φ_{fl} of **DPAP** in various solvents.

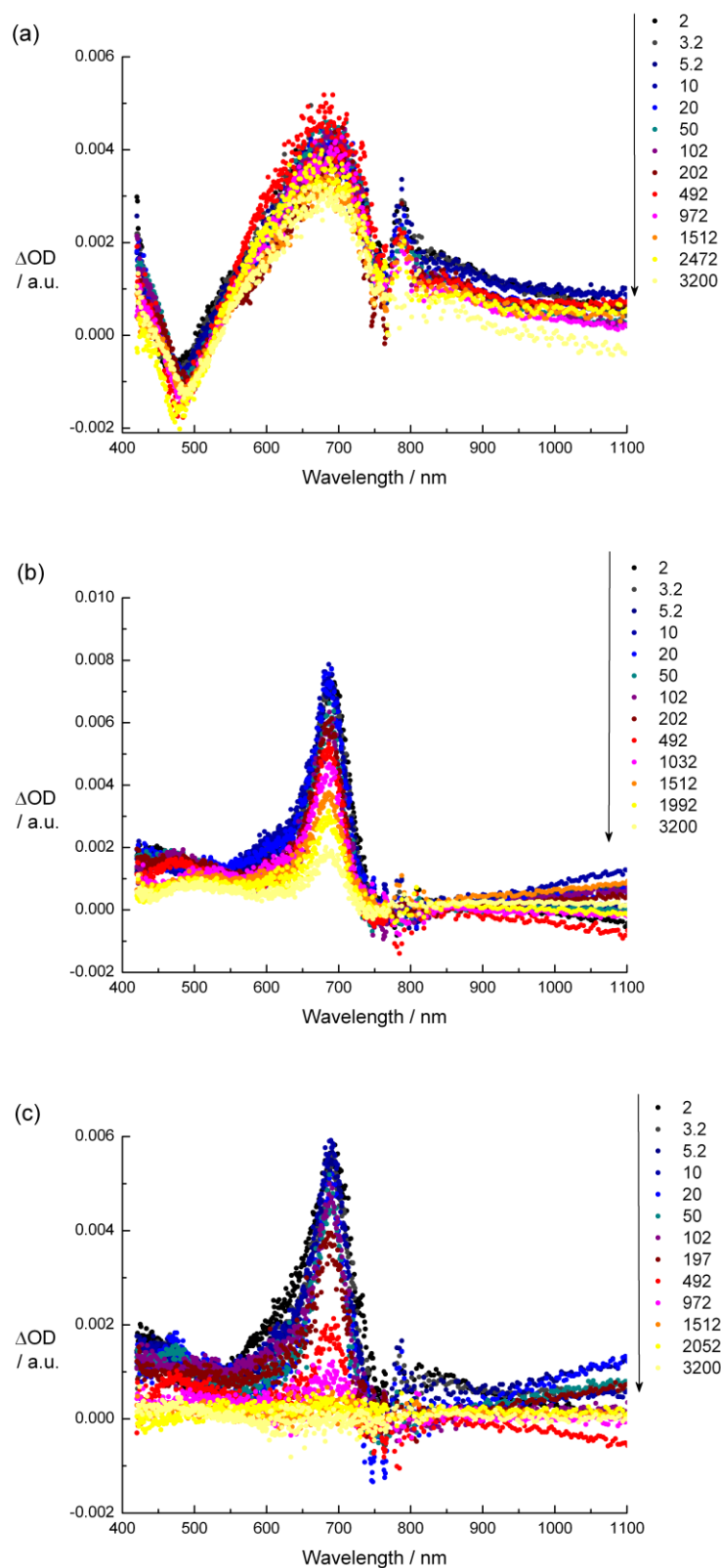


Fig. S5 Differential absorption spectra of DPAP obtained upon femtosecond flash photolysis in argon-saturated (a) *o*-xylene, (b) acetonitrile, and (c) methanol with several time delays between 0 and 3200 ps. OD at the 387 nm excitation wavelength was 0.2 - 0.3.

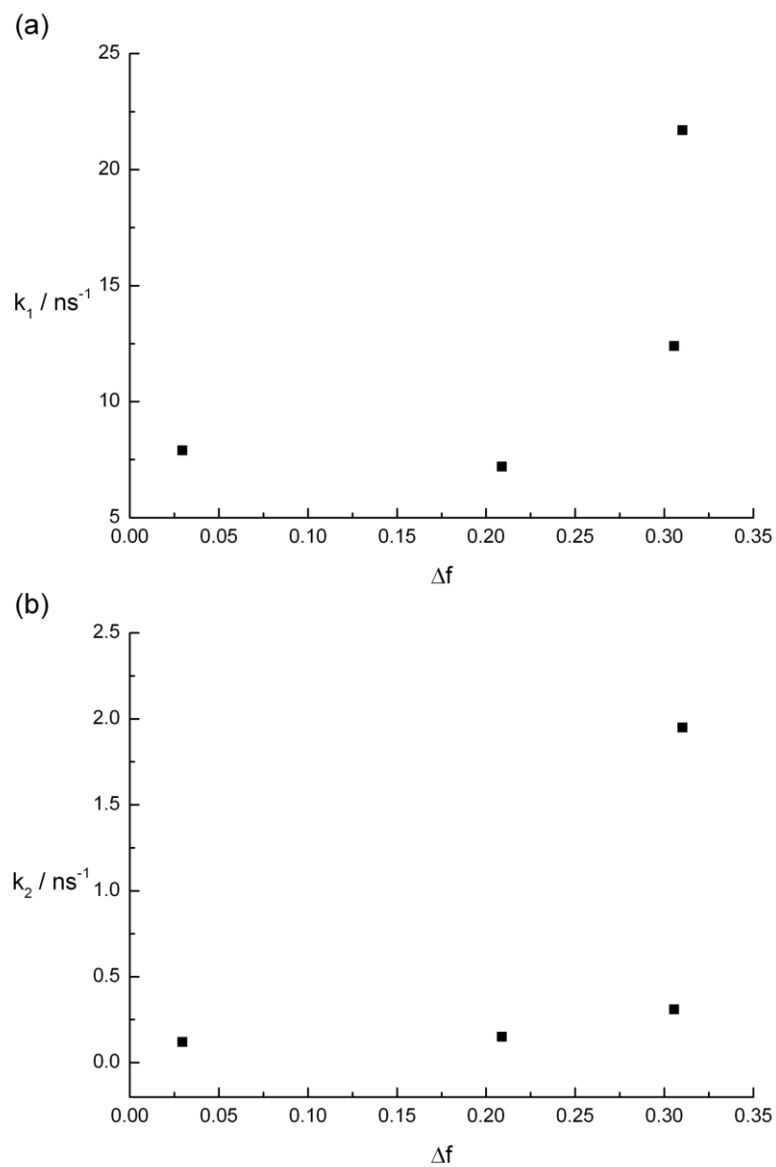


Fig. S6 Plot of the Lippert-Mataga solvent parameter Δf versus (a) the decay rate constant k_1 and (b) the decay rate constant k_2 for **DPAP** in argon-saturated *o*-xylene, THF, acetonitrile and methanol obtained upon femtosecond flash photolysis.

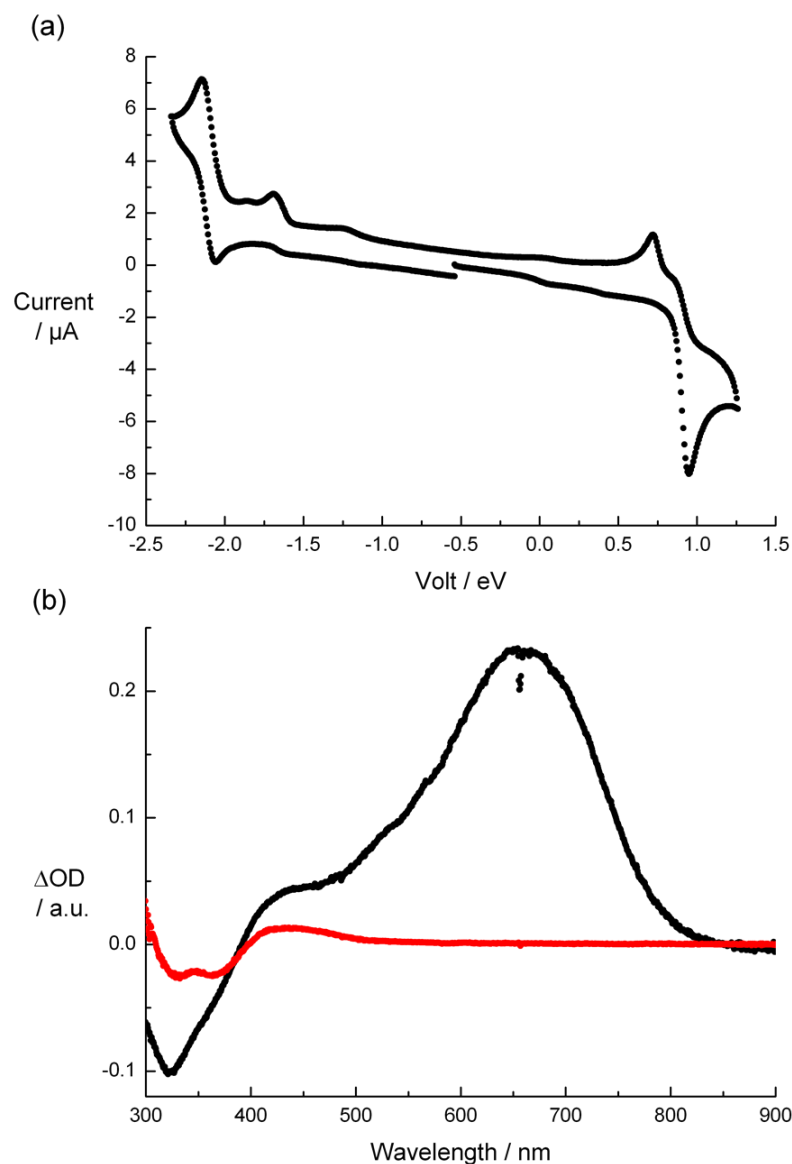


Fig. S7 (a) Cyclic voltammetry of **DPAP** (5×10^{-4} M) in acetonitrile vs Fc containing 0.1 M tetrabutylammonium hexafluorophosphate as supporting electrolyte. (b) Spectroelectrochemical spectra of **DPAP** (8×10^{-5} M) upon oxidation at +1.0 V vs Fc (black) and reduction at -2.1 V vs Fc (red) in acetonitrile containing 0.2 M tetrabutylammonium hexafluorophosphate as supporting electrolyte.

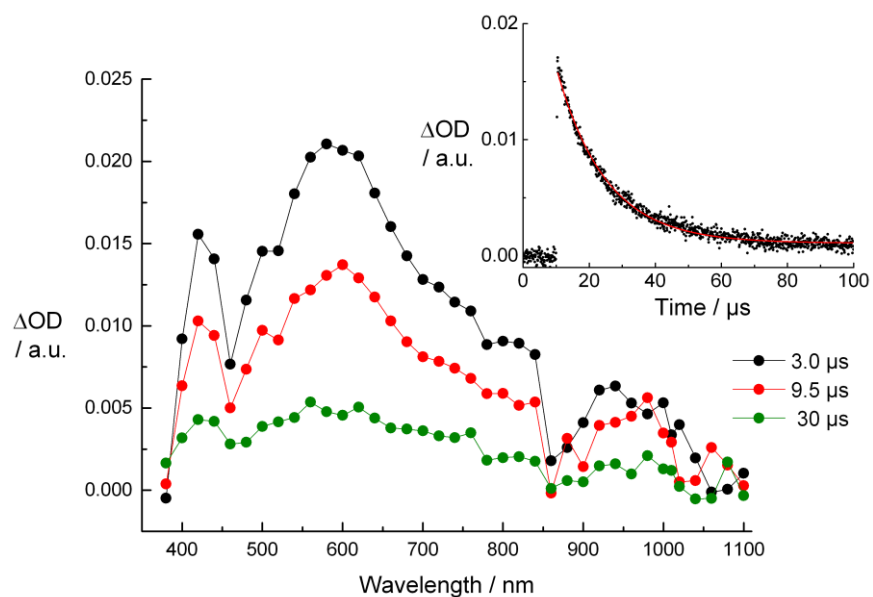


Fig. S8 Differential absorption spectra obtained upon nanosecond flash photolysis of **DPAP** in argon-saturated THF with different time delays. OD at the 355 nm excitation wavelength was 0.2. Inset: Corresponding time-absorption profile at 600 nm.

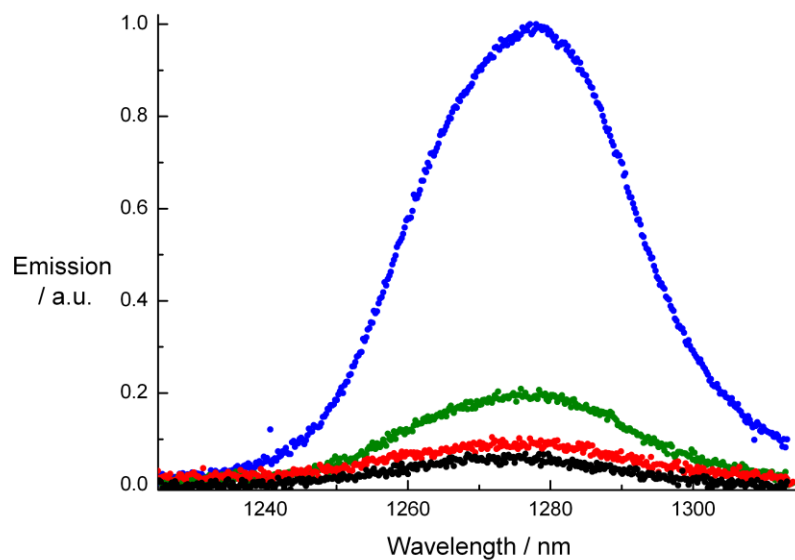


Fig. S9 Singlet oxygen phosphorescence spectra of **DPAP** in *o*-xylene (green), THF (red), and acetonitrile (black) as well as the reference free base tetraphenylporphyrin (blue) measured at room temperature in oxygen saturated solutions. OD at the excitation wavelength (403 nm) was 0.1 for all samples.

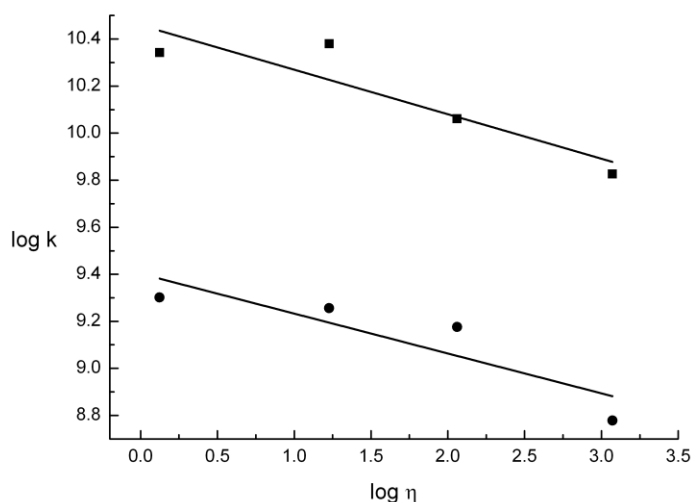


Fig. S10 Double-logarithmic plot of the solvent viscosity η versus the non-radiative decay constants k_1 (squares) and k_2 (circles) as determined from transient absorption spectroscopy for **DPAP** based on the Förster-Hoffmann equation.

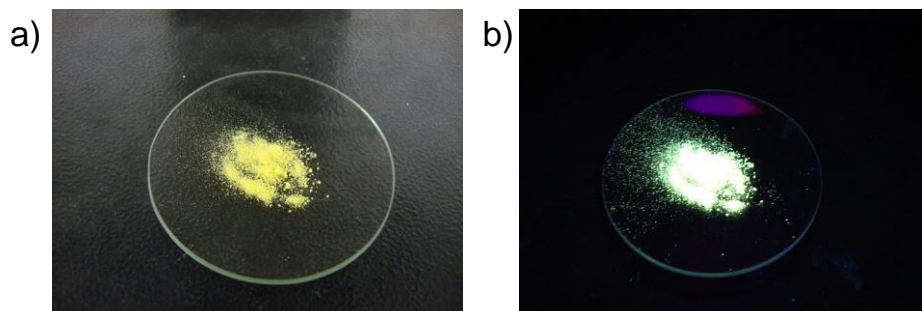


Fig. S11 Pictures of **DPAP** powder under a) light illumination and b) 365 nm UV illumination.

Table S4. Data collection and structure refinement for **DPAP**.

Empirical formula	C _{20.50} H ₁₃ Cl N ₃	
Formula weight	336.79	
Temperature	100(2) K	
Wavelength	1.54178 Å	
Crystal system	Triclinic	
Space group	P-1	
Unit cell dimensions	$a = 8.1851(4)$ Å	$\alpha = 94.129(5)^\circ$.
	$b = 8.5344(5)$ Å	$\beta = 99.175(4)^\circ$.
	$c = 13.5521(9)$ Å	$\gamma = 114.976(4)^\circ$.
Volume	$836.84(8)$ Å ³	
Z	2	
Density (calculated)	1.337 Mg/m ³	
Absorption coefficient	2.058 mm ⁻¹	

F(000)	348
Crystal size	0.25 x 0.15 x 0.08 mm ³
Theta range for data collection	3.34 to 67.37°.
Index ranges	-9<=h<=8, -9<=k<=10, -16<=l<=15
Reflections collected	9154
Independent reflections	2854 [R(int) = 0.0392]
Completeness to theta = 67.37°	94.8 %
Absorption correction	Semi-empirical from equivalents
Refinement method	Full-matrix least-squares on F ²
Data / restraints / parameters	2854 / 0 / 278
Goodness-of-fit on F ²	1.062
Final R indices [I>2σ(I)]	R1 = 0.0598, wR2 = 0.1613
R indices (all data)	R1 = 0.0663, wR2 = 0.1681
Largest diff. peak and hole	0.645 and -1.028 e·Å ⁻³

Supporting Information References

- 1 G. M. Sheldrick, SHELXL97, Program for the Refinement of Crystal Structures, University of Gottingen, Germany, 1994.
- 2 $R_w(F^2) = \{\sum w(|F_o|^2 - |F_c|^2)^2 / \sum w(|F_o|^4)\}^{1/2}$ where w is the weight given each reflection; $R(F) = \Sigma(|F_o| - |F_c|) / \Sigma|F_o|$ for reflections with $F_o > 4(\sigma(F_o))$; $S = [\sum w(|F_o|^2 - |F_c|^2)^2 / (n - p)]^{1/2}$, where n is the number of reflections and p is the number of refined parameters.
- 3 International Tables for X-ray Crystallography, Vol. C, Tables 4.2.6.8 and 6.1.1.4, ed. A. J. C. Wilson, Kluwer Academic Press, Boston, 1992.
- 4 (a) H. G. O. Becker, *Einführung in die Photochemie*, Georg Thieme Verlag, Stuttgart, 1983. (b) I. M. Smallwood, *Handbook of Organic Solvent Properties*, Elsevier, 1996. (c) M. Holdefer, *Relative Dielektrizitätskonstante εr (DK-Werte) von flüssigen und festen Medien*, Endress+Hauser Messtechnik GmbH+Co., Weil am Rhein, 1999. (d) N. P. Cheremisinoff, *Industrial Solvents Handbook*, 2nd edition, Princeton Energies Resources International, Rockville, Maryland, U.S.A., 2003. (e) N. S. Cheng, *Ind. Eng. Chem. Res.*, 2008, **47**, 3285–3288.
- 5 (a) E. Runge and E. K. U. Gross, *Physical Review Letters*, 1984, **52**, 997–1000. (b) M. E. Casida, Time-Dependent Density-Functional Response Theory for Molecules, in *Recent Advances in Density Functional Methods Volume 1*, ed. D. P. Chong, World Scientific, Singapore, 1995, pp 155–192.
- 6 (a) A. D. Becke, *J. Chem. Phys.*, 1993, **98**, 5648–5652. (b) P. J. Stephens, F. J. Devlin, C. F. Chabalowski and M. J. Frisch, *J. Chem. Phys.*, 1994, **98**, 11623–11627.
- 7 T. Yanai, D. P. Tew and N. C. A. Handy, *Chem. Phys. Lett.*, 2004, **393**, 51–57.
- 8 The SNST basis set is freely available online from the website: <http://dreamslab.sns.it/downloads>.

-
- 9 (a) A. Klamt and G. Schüürmann, *J. Chem. Soc., Perkin Trans. 2*, 1993, 799–805. (b) V. Barone and M. Cossi, *J. Chem. Phys. A*, 1998, **102**, 1995–2001. (c) M. Cossi, N. Rega, G. Scalmani and V. Barone, *J. Comput. Chem.*, 2003, **24**, 669–681.
- 10 R. Improta, V. Barone, G. Scalmani and M. J. Frisch, *J. Chem. Phys.*, 2006, **125**, 054103.
- 11 G. Scalmani, M. Frisch, B. Mennucci, J. Tomasi, R. Cammi and V. Barone, *J. Chem. Phys.*, 2006, **124**, 094107.
- 12 M. J. Frisch, G. W. Trucks, H. B. Schlegel, G. E. Scuseria, M. A. Robb, J. R. Cheeseman, G. Scalmani, et al. “Gaussian 09, Revision B.01,” 2009.
- 13 (a) E. Z. Lippert, *Naturforsch.*, 1957, **10a**, 541. (b) N. Mataga, Y. Kaifu and M. Koizumi, *Bull. Chem. Soc. Jpn.*, 1956, **29**, 465. (c) J. R. Lakowicz, *Principles of Fluorescence Spectroscopy*, Plenum Press, New York, 2006.